J|A|C|S
ARTICLES

Published on Web 07/01/2009

A Reduction Pathway in the Synthesis of PbSe Nanocrystal Quantum Dots

Jin Joo,[†] Jeffrey M. Pietryga,[†] John A. McGuire,[†] Sea-Ho Jeon,[†] Darrick J. Williams,[‡] Hsing-Lin Wang,[†] and Victor I. Klimov*[,†,‡]

Chemistry Division and Center for Integrated Nanotechnologies, Los Alamos National Laboratory, Los Alamos, New Mexico 87545

Received April 28, 2009; E-mail: klimov@lanl.gov

Abstract: Colloidal nanocrystal quantum dots (NQDs) of narrow band gap materials are of substantial general interest because of their unparalleled potential as infrared fluorophores. While PbSe NQDs are a promising class of infrared-active nanocrystals due to high emission quantum yields and a wide useful spectral range, typical synthetic methods are sensitive to a variety of factors, including the influence of solvent/ligand impurities that render reproducibility difficult. In this work, we specifically examine the effects of diphenylphosphine and 1,2-hexadecanediol, as surrogates for putative trioctylphosphine-based reducing impurities, on the synthesis of PbSe NQDs. Specifically, we compare their influence on NQD size, chemical yield, and photoluminescence quantum yield. While both additives substantially increase the chemical yield of the synthesis, they demonstrate markedly different effects on emission quantum yield of the product NQDs. We further examine the effects of reaction temperature and oleic acid concentration on the diol-assisted synthesis. Increased oleic acid concentration led to somewhat higher growth rates and larger NQDs but at the expense of lower chemical yield. Temperature was found to have an even greater effect on growth rate and NQD size. Neither temperature nor oleic acid concentration was found to have noticeable effects on NQD emission quantum yield. Finally, we use numerical simulations to support the conjecture that the increased yield is likely a result of faster monomer formation, consistent with the activation of an additional reaction pathway by the reducing species.

Introduction

Colloidally synthesized nanocrystal quantum dots (NQDs) have shown great promise as fluorophores suitable for a wide range of applications, including LEDs, lasers, detectors and optical labels, due to size-tunable band gaps and amenability to low-cost processing.[1−4] However, many important properties of colloidal NQDs critical to success in these applications, especially particle size and emission quantum yield (QY), are sensitive to growth conditions. Thus, the quality of fabricated NQDs depends on understanding of the growth dynamics during synthesis and how these dynamics are affected by parameters such as surface-capping ligand identity, precursor concentrations, and reaction temperature. In some cases, impurities typically found in common solvents and ligands, such as trioctylphosphine oxide,[5−8] have also been shown to have significant impact on particle size, shape, and QY, largely explaining observed inconsistencies in these qualities of NQDs synthesized by reported methods. In addition to empirical studies of the influence of such parameters as capping ligands on the chemical yield and corresponding photoluminescence (PL) QY,[8−12] the correlation between growth rate and QY in NQD ensembles has been modeled numerically by means of Monte Carlo simulations.[9,10] Commonly, and especially for the purposes of such simulations, the mechanism of colloidal NQD synthesis is described in terms of established colloid formation processes.[11] In short, molecular precursors are quickly injected into hot surfactant/solvent mixture and react to produce active "monomers". The rapid burst in concentration of these monomers creates a high supersaturation condition, which initiates nucleation of clusters or very small NQDs. As monomer concentration and temperature fall, the nucleated particles grow by addition of monomers or, when monomer concentration becomes low enough, by interparticle Ostwald ripening. In addition to modeling the growth and ripening processes, more recent numerical simulations have also included the reaction

[†] Chemistry Division.
[‡] Center for Integrated Nanotechnologies.

(1) Achermann, M.; Petruska, M. A.; Koleske, D. D.; Crawford, M. H.; Klimov, V. I. *Nano Lett.* **2006**, *6*, 1396–1400.
(2) Klimov, V. I.; Bawendi, M. G. *MRS Bull.* **2001**, *26*, 998–1004.
(3) Somers, R. C.; Bawendi, M. G.; Nocera, D. G. *Chem. Soc. Rev.* **2006**, *36*, 579–591.
(4) Medintz, I. L.; Tetsuo, H. U.; Goldman, E. R.; Mattoussi, H. *Nat. Mater.* **2005**, *4*, 435–436.
(5) Peng, X.; Manna, L.; Yang, W.; Wickham, J.; Scher, E.; Kadavanich, A.; Alivisatos, A. P. *Nature* **2000**, *404*, 59–61.
(6) Kawa, M.; Morii, H.; Ioku, A.; Saita, S.; Okuyama, K. *J. Nanopart. Res.* **2003**, *5*, 81–85.
(7) Kopping, J. T.; Patten, T. E. *J. Am. Chem. Soc.* **2008**, *130*, 5689–5698.
(8) Wang, F.; Tang, R.; Buhro, W. E. *Nano Lett.* **2008**, *8*, 3521–3524.
(9) Talapin, D. V.; Rogach, A. L.; Haase, M.; Weller, H. *J. Phys. Chem. B* **2001**, *105*, 12278–12285.
(10) Talapin, D. V.; Rogach, A. L.; Shevchenko, E. V.; Kornowski, A.; Haase, M.; Weller, H. *J. Am. Chem. Soc.* **2002**, *124*, 5782–5790.
(11) LaMer, V. K.; Dinegar, R. H. *J. Am. Chem. Soc.* **1950**, *72*, 4847–4854.
(12) Kwon, S. G.; Piao, Y.; Park, J.; Angappane, S.; Jo, Y.; Hwang, N.-M.; Park, J.-G.; Hyeon, T. *J. Am. Chem. Soc.* **2007**, *129*, 12571–12584.

10.1021/ja903445f CCC: $40.75 © **2009 American Chemical Society**

kinetics of monomer formation prior to particle nucleation, for example, in the specific case of iron oxide nanocrystals.[12] Studies of II−VI semiconductor NQDs in particular have elucidated key factors for high-level control over the growth not only of bright, stable spherical NQDs but also of shape-controlled particles such as nanorods,[5] tetrapods,[13] and nanoribbons.[14]

However, such studies have largely neglected the lead chalcogenides (PbE, where E = S, Se, or Te), despite the inherent importance of such infrared materials in telecommunications, biolabeling, and photovoltaics. Lead selenide (PbSe) is perhaps the most intriguing of these compounds. With a narrow bulk band gap (0.26 eV) and large exciton Bohr radius (46 nm), PbSe NQDs can exhibit very strong quantum confinement: colloidal syntheses of PbSe NQDs with size-tunable emission spanning from 0.3 to 1.4 eV are known, and QYs approaching unity are well-established in the near-infrared, including at the telecommunications window at 0.8 eV. While for many applications visible-emitting (e.g., CdSe) NQDs are posited as superior replacements for existing solution-processible technologies such as organic dyes, PbSe NQDs represent a fundamentally new capability: there are *no existing competing fluorophores* within this energy range. Moreover, PbSe NQDs were the first to exhibit carrier multiplication, or direct generation of more than one electron−hole pair from a single absorbed photon, an effect that could lead to photovoltaic power conversion efficiencies in excess of the Schockley−Queisser limit.[15−18]

High QY PbSe NQDs of a large range of sizes can be synthesized by reaction of lead oleate and trioctylphosphine selenide (TOPSe), but this method is not without its shortcomings. The reaction can be quite sensitive to small changes in conditions, and thus consistency is still an issue. For example, trace amounts of acetate ion from lead acetate precursor, unremoved, can have dramatic effects on PbSe NQD size and shape.[19] In addition, sample to sample variations in ligand coverage have been proposed to result in an unpredictable distribution of charges in PbSe NQD ensembles.[20] One of the biggest limitations, as occasionally noted,[21] is that typical PbSe NQD syntheses produce fairly low chemical yields, especially for smaller particle sizes. Recently, Steckel et al. reported that adding diphenylphosphine (DPP) to the reaction can greatly improve chemical yields.[22] A surrogate for potential dialkylphosphine impurities found in trioctylphosphine (TOP), especially in ∼90% pure technical TOP used in most studies, DPP was posited to act as a reducing agent to produce Pb^0 species, resulting in two possible pathways to [PbSe] monomer formation.

$$(R_aCOO)_2Pb + Se{=}P(R_b)_3 \rightarrow [PbSe] + O{=}P(R_b)_3 + (RCO)_2O \quad (1)$$

$$(R_aCOO)_2Pb + PH(R_c)_2 \rightarrow [Pb^0] + O{=}PH(R_c)_2 + (R_aCO)_2O$$
$$[Pb^0] + Se{=}P(R_b)_3 \rightarrow [PbSe] + P(R_b)_3 \quad (2)$$

The combination of two mechanisms was proposed to result in faster monomer supersaturation, resulting in a larger nucleation event (i.e., a larger number of particles formed) and the observed high chemical yield.

Unmentioned, though, is the effect of DPP on PL QY. The present study supports our previous report that dialkyl- or diarylphosphines often have deleterious effects on emission efficiency[23] and further finds that NQD size control can be difficult to achieve in this system because of the very fast reaction rate. To overcome these difficulties and to verify the existence of two reaction pathways, we employ the alternative reducing agent 1,2-hexadecanediol (HDD) in the synthesis of PbSe NQDs. According to its use in the "polyol method" for production of fine metal powders, HDD might be expected to produce Pb^0 species with aldehyde side products (eq 3).

$$(R_aCOO)_2Pb + HDD \rightarrow [Pb^0] + HC(=O)R + HC(=O)H + 2R_aCOOH$$
$$[Pb^0] + Se{=}P(R_b)_3 \rightarrow [PbSe] + P(R_b)_3 \quad (3)$$

We find that, by using HDD, high chemical yields can be achieved without effect on PL QY or loss of fine control over particle size. We then study the effects of temperature and ligand (oleic acid) concentration on the new system, toward developing a rational, reproducible high-yield synthesis for PbSe NQDs at a range of sizes. Finally, we compare our reaction time profiles to the results of numerical simulations to confirm that the enhanced chemical yield can indeed be the result of the contributions of an additional monomer formation mechanism.

Experimental Section

General Considerations. All syntheses were performed under exclusion of air and moisture using standard Schlenk techniques up until reaction quenching. Postpreparative handling and spectroscopy were conducted under ambient conditions. Lead(II) acetate trihydrate ($Pb(OAc)_2 \cdot 3H_2O$, Aldrich, 99.99+%), selenium shot (Alfa Aesar, 99.999%), oleic acid (OA, Aldrich, 90%), 1-octadecene (ODE, Aldrich, 90%), chloroform-*d* (Aldrich, 99.9 atom % D) were used as received without further purification. Trioctylphosphine (TOP, Aldrich, 90%) was purified by evaporation of volatile, low molecular weight compounds at 160 °C under dynamic vacuum for 4−8 h. 1,2-Hexadecanediol (HDD, Aldrich, 90%) was purified by dissolution in diethyl ether, followed by filtration through paper to remove insoluble species and drying under vacuum. A 0.4 M TOPSe stock solution was prepared by stirring an appropriate amount of Se shot in TOP overnight at room temperature in an inert atmosphere glovebox.

Synthesis of PbSe NQDs Using HDD. $Pb(OAc)_2 \cdot 3H_2O$ (0.38 g, 1 mmol) and OA (0.95 mL, 3 mmol) were added to 10 mL of ODE and heated to 100 °C for 3 h under vacuum to prepare lead oleate and remove acetic acid completely. Concurrently, 20 mL of ODE containing the appropriate amount of HDD was heated at 100 °C under vacuum for degassing and drying. The ODE/HDD

(13) Manna, L.; Scher, E. C.; Alivisatos, A. P. *J. Am. Chem. Soc.* **2000**, *122*, 12700–12706.
(14) Joo, J.; Son, J. S.; Kwon, S. G.; Yu, J. H.; Hyeon, T. *J. Am. Chem. Soc.* **2006**, *128*, 5632–5633.
(15) Nozik, A. J. *Annu. Rev. Phys. Chem.* **2001**, *52*, 193–231.
(16) Schaller, R. D.; Klimov, V. I. *Phys. Rev. Lett.* **2004**, *92*, 186601–186604.
(17) Klimov, V. I. *J. Phys. Chem. B* **2006**, *110*, 16827–16845.
(18) McGuire, J. A.; Joo, J.; Pietryga, J. M.; Schaller, R. D.; Klimov, V. I. *Acc. Chem. Res.* **2008**, *41*, 1810–1819.
(19) Houtepen, A. J.; Koole, R.; Vanmaekelbergh, D.; Meeldijk, J.; Hickey, S. G. *J. Am. Chem. Soc.* **2006**, *128*, 6792–6793.
(20) Shevchenko, E. V.; Talapin, D. V.; Kotov, N. A.; O'Brien, S.; Murray, C. B. *Nature* **2006**, *439*, 55–59.
(21) Yu, W. W.; Falkner, J. C.; Shih, B. S.; Colvin, V. L. *Chem. Mater.* **2004**, *16*, 3318–3322.
(22) Steckel, J. S.; Yen, B. K. H.; Oertel, D. C.; Bawendi, M. G. *J. Am. Chem. Soc.* **2006**, *128*, 13032–13033.
(23) Pietryga, J. M.; Werder, D. J.; Williams, D. J.; Casson, J. L.; Schaller, R. D.; Klimov, V. I.; Hollingsworth, J. A *J. Am. Chem. Soc.* **2008**, *130*, 4879–4885.

was then heated under argon to 160 °C, and 5 mL of 0.4 M of TOPSe stock solution was added to the lead oleate solution, which was then rapidly injected into the ODE/HDD. Temperature was allowed to decrease and was stabilized at 120 °C. NQD growth was monitored by analysis of 1−2 mL aliquots removed at various times during the reaction. In each case, PbSe NQD solids were precipitated by addition of excess ethanol, centrifuged, separated from the decantate, rinsed with acetone, and redispersed in hexane. The precipitation/redispersion procedure was repeated two times, and then the product was dried under vacuum. Spectroscopic analysis was performed on solutions of NQDs in a measured amount of chloroform-*d* (1−5 mL in order to bring the solution optical density below 0.1 at 808 nm), after filtering through a 200 nm PTFE-membrane syringe filter to remove any insoluble species.

Synthesis of PbSe NQDs Using DPP. The synthesis was carried out in an identical manner, with the exception of omitting HDD, and adding the appropriate amount of DPP to the 0.4 M TOPSe stock solution prior to mixing with lead oleate.

Temperature and OA Concentration Studies. To determine the effects of temperature or OA concentration on growth, the same general synthesis, using 1.0 g (4 mmol) of HDD, was varied appropriately. For the temperature studies, growth temperatures were stabilized at a common temperature close to that reached by the solution naturally as a result of the injection. For injections at 160 °C, NQDs were grown at 120 °C. Injections at 200 °C corresponded to 150 °C growth, and 240 °C injections to 180 °C growth.

Study of the Reaction between Pb(oleate)$_2$ and HDD. To confirm the ability of HDD to reduce Pb^{2+} to Pb^0, a mixture of 10 mmol of HDD and 10 mmol of Pb(oleate)$_2$ was heated to 200 °C for 1 h under Ar flow. Volatile byproducts of the reaction were collected by bubbling into chilled deuterium oxide contained in an NMR tube and analyzed by ^{1}H NMR spectroscopy. The gray solids were retrieved from the reaction flask, rinsed with acetone, and identified by X-ray diffraction (XRD) analysis.

Characterization Methods. UV−vis−NIR absorption spectra on PbSe NQD solutions were collected from a Perkin-Elmer Lambda-950 spectrophotometer. Mean NQD diameters were determined from the energy of the 1S absorption maxima, according to an established sizing curve.[24] Chemical yields were calculated on the basis of NQD concentrations, n_{NQD}, derived from the optical densities, OD, at 400 nm of solutions prepared from reaction aliquots using the expression $n_{NQD} = \mathrm{OD}\ \ln(10)/S_a$, where S_a is an NQD absorption cross section at 400 nm. Absorption cross sections were calculated based on the bulk PbSe absorption coefficient, α_0,[25] scaled by the NQD volume, V_0, and the local-field-correction factor, η:[26] $S_a = \alpha_0(n_b/n_{sol})V_0|\eta|^2$, where n_b and n_{sol} are the refractive indices of bulk PbSe and NQD solvent, respectively. This method was established previously to yield values in good agreement with those determined by more direct measurements involving elemental analysis.[24] The growth solution concentrations were back-calculated from the sample concentrations using the dilution volume and the total volume of the aliquot taken.

PL spectra were taken with an excitation of 808 nm diode laser and an LN_2-cooled InSb detector with a grating monochromator. The excitation was mechanically chopped, and the signal was enhanced by a lock-in amplifier. NQD PL QY was calculated using IR26 laser dye as a standard with a QY of 0.5%, and corrections for grating and detector efficiencies were conducted before QY calculation.

^{1}H NMR data and ^{31}P NMR data were acquired on Bruker 400 MHz spectrometer operating at 400 and 161 MHz, respectively. ^{31}P NMR was referenced to external phosphoric acid standard.

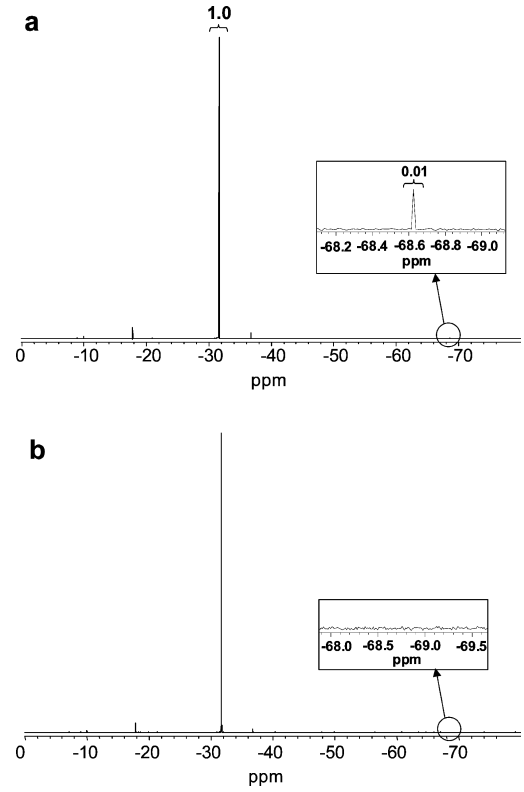

Figure 1. ^{31}P NMR spectra of TOP in toluene (a) before and (b) after purification at 160 °C under vacuum for 8 h. The chemical shifts of TOP and dialkylphosphine are −31.66 and −68.63 ppm, respectively. As can be seen in the insets, the small dialkylphosphine peak is absent after purification.

XRD was performed on a Philips D-5000 diffractometer using Cu Kα radiation source (0.15418 nm).

Results and Discussion

For the purposes of this study, we chose to modify the basic synthetic procedure as reported by Murray et al.[27] and then elaborated upon by other groups. In addition to the variables under study (TOP purity and reducing agents, OA concentration, temperature), one notable change was to substitute ODE for the originally used phenyl ether. The relatively low boiling point of phenyl ether makes it difficult to sufficiently heat the reaction mixture under vacuum during lead oleate preparation in order to drive off water and acetic acid without losing solvent. ODE, which has been successfully used in previous PbSe NQD synthesis reports, has a higher boiling point that allows more thorough drying of the lead oleate solution to yield more consistent size control.

Role of TOP Impurities and Reducing Agents. As mentioned above, because they are reducing agents, dialkylphosphines have been identified as the most likely active TOP impurities, possibly responsible for the universally acknowledged (if rarely published) batch-to-batch variation in PbSe NQD syntheses. Figure 1a shows a ^{31}P NMR spectrum of as-received technical-grade TOP, which is found to contain approximately 1% (molar) of dialkylphosphine impurity, likely dioctylphosphine. At this level, the 5 mL of TOP used in our experiment would contain roughly 0.1 mmol dioctylphosphine, or enough to reduce up to 10% of the lead according to eq 2. In order to probe its effect on

(24) Moreels, I.; Lambert, K.; De Muynck, D.; Vanhaecke, F.; Poelman, D.; Martins, J. C.; Allan, G.; Hens, Z. *Chem. Mater.* **2007**, *19*, 6101–6106.
(25) Suzuki, N.; Sawai, K.; Adachi, S. *J. Appl. Phys.* **1995**, *77*, 1249–1255.
(26) Klimov, V. I. *J. Phys. Chem. B* **2000**, *104*, 6112–6123.
(27) Murray, C. B.; Sun, S.; Gaschler, W.; Doyle, H.; Betley, T. A.; Kagan, C. R *IBM J. Res. Dev.* **2001**, *45*, 47–56.

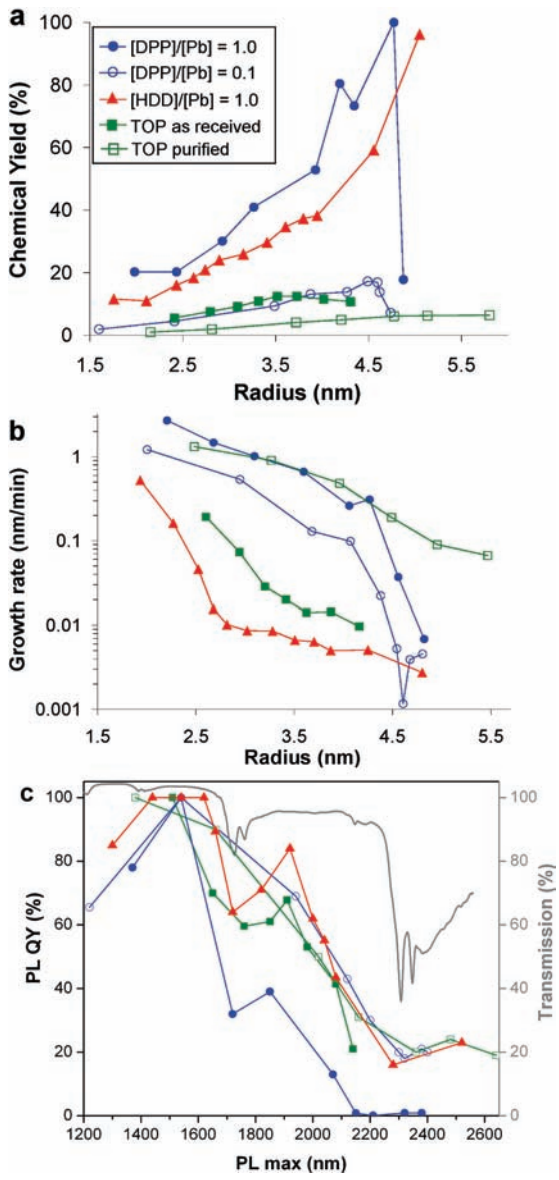

Figure 2. Effect of reducing agents during synthesis of PbSe NQDs. (a) Chemical yield and (b) growth rate of PbSe NQDs as a function of average radius. The rapid decline in yield for high-DPP synthesis (blue closed circles) is due to precipitation. (c) PL QY of corresponding PbSe NQDs overlaid with the near-IR transmission spectrum of oleic acid (TOP is very similar). The injection temperature for all samples was 200 °C, and the [OA]/[Pb] ratio was fixed at 3.

synthesis, we endeavored to remove this impurity. The lower boiling point of dioctylphosphine suggests it might be accomplished by evaporation, and indeed, after 4−8 h under dynamic vacuum at 160 °C, the corresponding peak is no longer found in the ^{31}P NMR spectrum (Figure 1b), although peaks corresponding to other impurities remain largely unchanged.

We studied the effect of this inherent TOP impurity on chemical yield and QY by synthesizing PbSe NQDs using TOP both before and after purification, maintaining other synthetic conditions the same. Figure 2a shows chemical yield as a function of size as the particles grow. In both cases, chemical yield increases with size up to a certain size, at which it levels off as a result of Ostwald ripening. In this process, small NQDs with high surface potential dissolve away and larger NQDs are supplied with monomers at the expense of smaller ones, leading to no net increase in yield.[5,44] TOP before purification achieves a maximum yield of 12% at 3.5 nm of radius, while purified TOP yields are roughly one-third as high over the whole radius range before leveling off at a larger radius of 5.0 nm. When DPP, as a commercially available surrogate for the dialkylphosphine impurities, is added to the purified TOP at a level comparable to the original impurities ([DPP]/[Pb] = 0.1), chemical yields are similar to the as-received (unpurified) TOP. By adding more DPP, in excess of typical impurity levels, it is possible to reach even higher yields; in fact, as Figure 2a shows, when [DPP]/[Pb] = 1.0, yield can reach essentially 100%. DPP also markedly increases the growth rate, as shown in Figure 2b. While this allows larger sizes to be achieved without noticeable ripening, evidence suggests this may be at the expense of NQD quality. At sizes above 4.5 nm in radius, a large fraction of the NQD solid precipitates are no longer dispersible in organic solvents, which is the cause of the precipitous drop in chemical yield (as determined spectroscopically on filtered samples). Poor dispersibility is not endemic to NQDs of this size: NQDs with radii in excess of 8 nm have been synthesized previously without such dramatic loss of solubility.[28]

NQD quality can also be judged by PL QY (shown in Figure 2c). Regardless of the presence of impurities or DPP, all syntheses demonstrate the established trend in which QY declines as emission wavelength increases. The interruptions in this monotonic trend near 1700 and 2300 nm are a result of reabsorbance of PL by the organic surface ligands. The correlation between QY and emission wavelength is nearly identical for all of the low-yield syntheses. However, the single high-yield synthesis using a larger amount of DPP resulted in an earlier (i.e., at lower wavelengths) and more dramatic decline, eventually falling below 1% before reaching the sizes at which the NQDs are no longer dispersible. The combination of low QY and poor dispersibility implies that the quality of the NQDs may suffer as a result of fast growth, possibly as a result of limited surface reorganization due to short growth times and modest growth temperatures. In addition, DPP itself is highly air-sensitive; any residual DPP on the NQD surfaces after reaction can be expected to have a destabilizing effect. Thus, the use of DPP for enhancing chemical yield limits both PL QY as well as the range of usable sizes.

While DPP itself does not solve the dilemma of efficient synthesis of high-quality NQDs, it certainly suggests that use of a reducing agent may be the answer. To test this conjecture, we employed HDD as an alternative to DPP (eq 3). 1,2-Diols are established reducing agents, especially in the synthesis of metal nanocrystals,[29−36] but are considerably less reactive than dialkylphosphines. HDD was chosen because of its solubility in nonpolar solvents and high boiling point. HDD has also been used in the synthesis of cadmium selenide nanocrystals.[37−39] In order to prove that HDD would act as a reducing agent toward

(28) Pietryga, J. M.; Schaller, R. D.; Werder, D.; Stewart, M. H.; Klimov, V. I.; Hollingsworth, J. A. *J. Am. Chem. Soc.* **2004**, *126*, 11752–11753.
(29) Fiévet, F.; Lagier, J. P.; Blin, B.; Beaudoin, B.; Figlarz, M. *Solid State Ionics* **1989**, *32−33*, 198–205.
(30) Toshima, N.; Yonezawa, Y. T. *New J. Chem.* **1998**, *22*, 1179–1201.
(31) Teranishi, T.; Miyake, M. *Chem. Mater.* **1998**, *10*, 594–600.
(32) Lu, P.; Teranishi, T.; Asakura, K.; Miyake, M.; Toshima, N. *J. Phys. Chem. B* **1999**, *103*, 9673–9682.
(33) Sun, S.; Murray, C. B.; Weller, D.; Folks, L.; Moser, A. *Science* **2000**, *287*, 1989–1992.
(34) Murray, C. B.; Sun, S.; Doyle, H.; Betley, T. A. *MRS Bull.* **2001**, *26*, 985–991.
(35) Sun, Y.; Xia, Y. *Science* **2002**, *298*, 2176–2179.
(36) Kim, F.; Connor, S.; Song, H.; Kuykendall, T.; Yang, P. *Angew. Chem., Int. Ed.* **2004**, *43*, 3673–3677.
(37) Bawendi, M. G.; Stott, N. E. U.S. Patent 6,576,291, 2003.

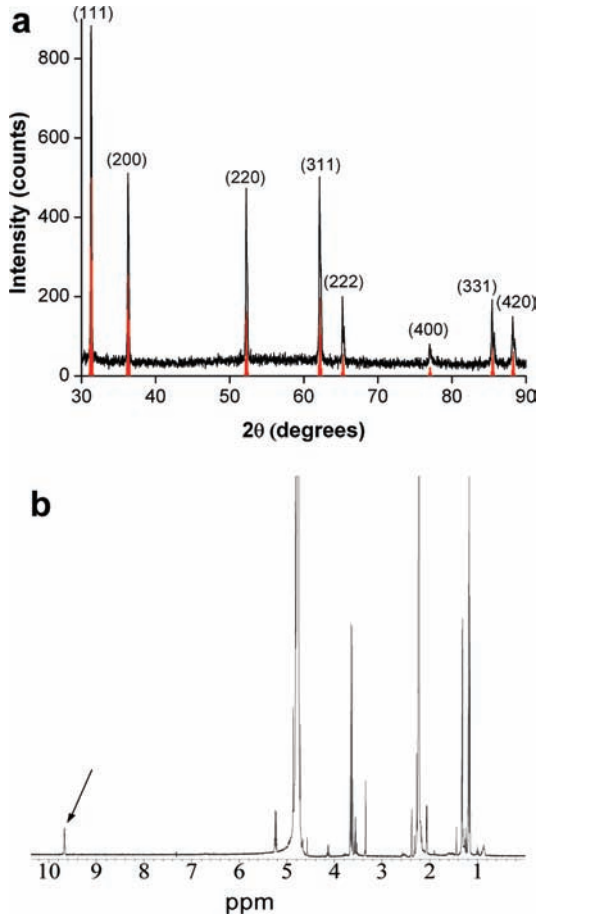

Figure 3. Identification of the products from the reaction of $Pb(oleate)_2$ and HDD. (a) Powder XRD pattern of gray solids (black) compared to the pattern of fcc Pb metal (red). (b) ^1H NMR spectrum of volatile products, confirming formation of aldehydes (arrow, $\delta = 9.7$ ppm).

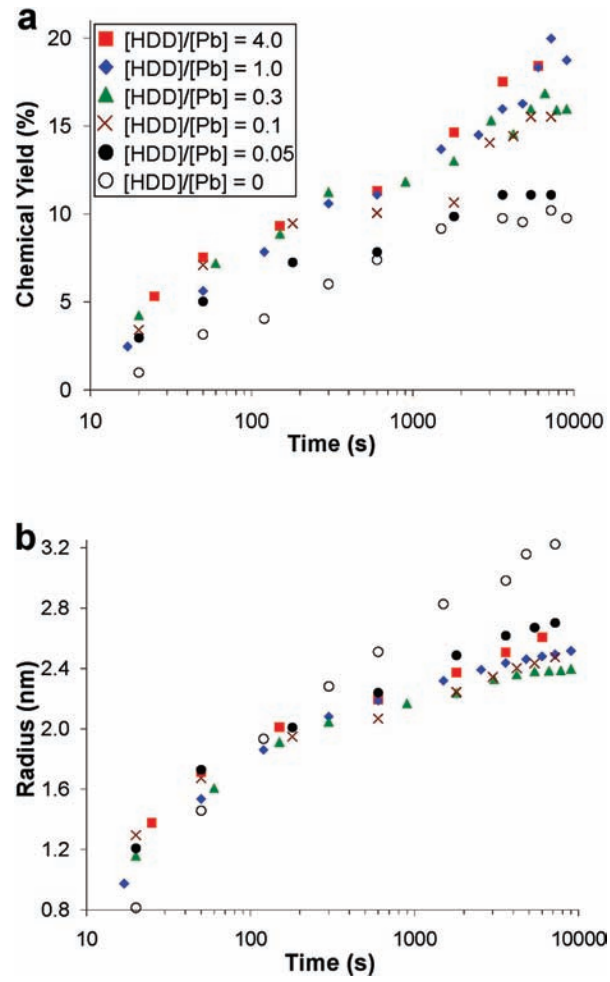

Figure 4. Effect of HDD concentration on the growth of PbSe NQDs. (a) Chemical yield as a function of time. (b) Radius evolution over time. The injection temperature for all samples was 160 °C, and the [OA]/[Pb] ratio was fixed at 3.

lead ions under typical reaction conditions, in a preliminary experiment, a mixture of $Pb(oleate)_2$ and HDD was heated under argon. As the temperature increased to 160 °C, the colorless reaction mixture began to turn green, accompanied by the liberation of a gas, and eventually a large amount of gray solid material appeared. The solid was identified as lead metal by XRD analysis (Figure 3a). The reaction likely proceeds along a mechanism similar to that observed in the oxidative cleavage of vicinal diols by $Pb(OAc)_4$ to produce aldehydes and $Pb(OAc)_2$.[40] To check for the presence of aldehydes (such as formaldehyde), the volatile products of this reaction were carried by argon flow into a deuterium-oxide-filled NMR tube "trap". ^1H NMR spectroscopy of the resulting solution confirms the presence of aldehydes (Figure 3b).

The synthesis of PbSe NQDs with HDD ([HDD]/[Pb] = 1.0) shows chemical yield enhancement similar to that produced by DPP, peaking at a slightly larger size (Figure 2a), but the largest NQDs do not suffer from any loss of dispersibility. Moreover, HDD-synthesized NQDs have higher QYs, especially at larger sizes (Figure 2c). The gains in quality are likely the result of the slower growth rate (Figure 2b), which also means size control is much easier, as the consequences of errors involved in reaction quenching are less severe. Interestingly, above a threshold of ~0.1, chemical yield of PbSe NQDs is largely insensitive to [HDD]/[Pb] ratio (Figure 4a). Below this point, however, chemical yield is lower throughout the course of reaction. This is a result of a smaller number of nanoparticles formed at the nucleation event (a small nucleation event). Fewer particles means more precursors available in solution after nucleation, which in turn leads to a faster growth rate of individual particles and larger average NQD size (Figure 4b).

Effect of OA Concentration on Nucleation with HDD. The large nucleation event in reactions using a reducing agent like HDD influences the way the particle growth dynamics change over the course of the whole reaction. It is therefore worth investigating the effects of common factors, such as capping ligand concentration and temperature, on growth under these new conditions. To elucidate the effect of OA concentration on growth dynamics, [OA]/[Pb] ratio was varied from 2.2 to 15 at a constant injection temperature of 160 °C (growth at 120 °C) and [HDD]/[Pb] ratio of 4. At a first glance, increasing OA concentrations lead to generally lower NQD concentrations (and consequently lower yields) when considered either in terms of time (Figure 5a) or particle size (Figure 5b). Thus, it seems that OA has an effect on the nucleation event opposite to that

(38) Jarosz, M. V.; Stott, N. E.; Drndic, M.; Morgan, N. Y.; Kastner, M. A.; Bawendi, M. G. *J. Phys. Chem. B* **2003**, *107*, 12585–12588.
(39) Halpert, J. E.; Porter, V. J.; Zimmer, J. P.; Bawendi, M. G. *J. Am. Chem. Soc.* **2006**, *128*, 12590–12591.
(40) Moriconi, E. J.; O'Connor, W. F.; Keneally, E. A.; Wallenberger, F. T. *J. Am. Chem. Soc.* **1960**, *82*, 3122–3126.

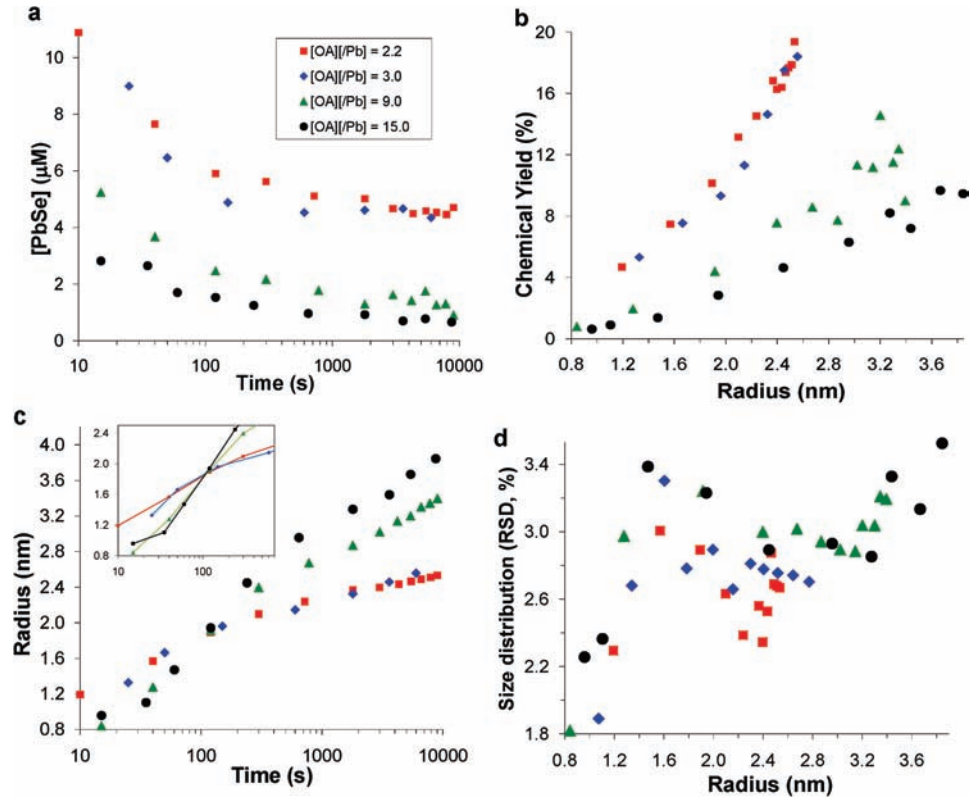

Figure 5. Effect of OA concentration on PbSe NQD growth dynamics. (a) Evolution of NQD concentration during the reaction for four OA concentrations. (b) Variation of chemical yield with size during growth of the same NQDs. (c) Size vs reaction time, with the unusual "crossover" behavior highlighted in the inset (lines added as a guide to the eye). (d) Size distribution of the corresponding NQDs as a function of size, expressed as relative standard deviation (RSD) of the particle radius. This measure of size dispersity was derived from the PL spectra using the following equation: RSD = 0.21 × fwhm/(λ_{max} − 0.26), where λ_{max} is the measured PL peak energy, fwhm is the full width at half-maximum of the PL peak, and 0.26 is the bulk band gap of PbSe. Injection temperature for all samples is 160 °C at the ratio of [HDD]/[Pb] = 4.

of reducing agents like HDD. This implies that, in large concentrations, OA suppresses monomer formation.

More evidence of this can be seen in Figure 5c, in which we can see unique "crossover" behavior in the growth traces of high- and low-OA reactions. At high OA levels, slow monomer formation means that growth lags at early reaction times, even though the smaller number of particles means much higher levels of unreacted precursors overall. Eventually, monomer levels match and then exceed those found in low-OA reactions, leading to relatively faster growth and larger particles at late times. Although this observed size dependence on OA concentration stands in contrast to a previous PbSe report,[41] it is in good qualitative agreement with the reported trend for PbTe NQDs,[42] which, ironically, might be a more apt comparison for our system. In HDD-assisted synthesis, monomer formation is a much faster process than in typical syntheses; the same can be said for PbTe synthesis using the more reactive TOPTe (relative to TOPSe). In the case of HDD-assisted synthesis, the reduction of lead ions required to open the second monomer formation pathway can be inhibited by OA. In the most straightforward sense, reduction of lead ions requires initial complex formation between the diol functionality and the lead center. As the concentration of OA increases, this complex formation may be competitively inhibited in favor of the stronger-donating, chelating OA (or oleate ions), effectively shutting down the reductive pathway. The result is a return to a more typically sized nucleation event (fewer particles) and, consequently, low chemical yield. The slow kinetics observed in high-OA syntheses could also be expected to spread the nucleation event out in time, as the onset and conclusion of the supersaturation condition becomes less discrete due to less abrupt changes in monomer concentration. Evidence that this is indeed the case can be seen in Figure 5d, in which we can see that, for all sizes, size distributions (as determined from PL peak width) for NQDs synthesized with high-OA concentrations are broader, indicating a less discrete, more prolonged nucleation event.

Effect of Injection Temperature on Nucleation with HDD. Increasing the injection and growth temperature of the PbSe NQD synthesis has been shown experimentally to increase growth, leading to larger particles at short times.[27,28] On the other hand, previously reported numerical simulations predict that higher injection temperatures should increase the degree of supersaturation at the nucleation stage, leading to high NQD concentrations, lower monomer concentrations after nucleation, and ultimately smaller particles.[9,43] In the present study, the inherently larger nucleation event in reactions with HDD should result in lower monomer concentrations throughout growth even

(41) Moreels, I.; Fritzinger, B.; Martins, J. C.; Hens, Z. *J. Am. Chem. Soc.* **2008**, *130*, 15081–15086.
(42) Urban, J. J.; Talapin, D. V.; Shevchenko, E. V.; Murray, C. B. *J. Am. Chem. Soc.* **2006**, *128*, 3248–3255.
(43) Park, J.; Joo, J.; Kwon, S. G.; Jang, Y.; Hyeon, T. *Angew. Chem., Int. Ed.* **2007**, *46*, 4630–4660.
(44) Fitting is carried out with the reaction rate constant of $k_1 = 5.0 \times 10^{-2}$ L mol s^{-1}, $k_2 = 4.0 \times$ L$^{0.1}$ mol$^{-0.1}$ s^{-1}, and $k_3 = 10.0$ L mol s^{-1}. The power in eqs 6, 7, and 8 is set at $\alpha_1 = 1.0$, $\beta_1 = 1.0$, $\alpha_2 = 1.0$, $\beta_2 = 1.0$, $\alpha_3 = 1.0$, and $\beta_3 = 1.0$. The initial concentration of precursors accords with experimental condition, e.g., [Pb] = 2.83 M, [Se] = 5.66 M, and [HDD] = 0.283 M, respectively.

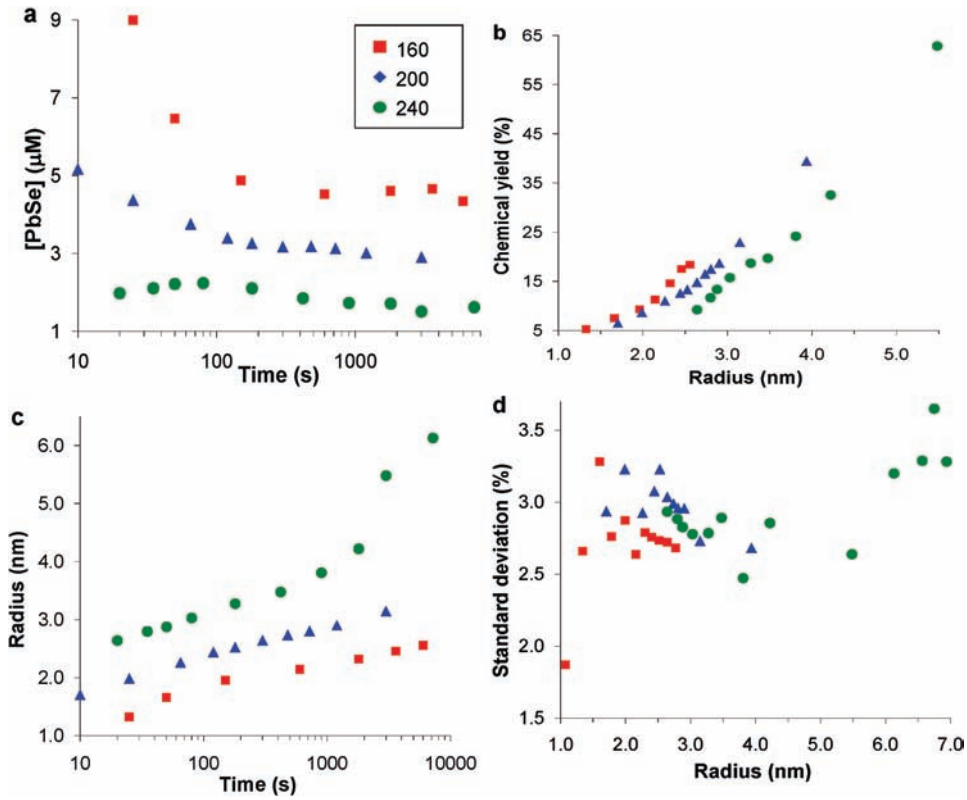

Figure 6. PbSe NQD growth dynamics at three injection temperatures. (a) Evolution of NQD concentration during the reaction. (b) Variation of chemical yield with size during growth of the same NQDs. (c) Size vs reaction time. (d) Size distribution of the corresponding NQDs as a function of size, expressed as RSD of the particle radius. In all reaction, the ratios of [OA]/[Pb] and [HDD]/[Pb] were 3 and 4, respectively.

at lower temperatures, so the effect of temperature is not necessarily clear a priori.

Experiments were carried out at injection temperatures of 160, 200, and 240 °C at [OA]/[Pb] = 3 and [HDD]/[Pb] = 4. We focus on injection temperature more than growth temperature because we find that growth dynamics of NQDs are strongly related to conditions during nucleation, which determines the number of particles formed. Empirically, the effects of increasing the temperature are similar to those of increasing OA concentration but, in some respects, are much more pronounced. In Figure 6a,b, we see that initial and final NQD concentrations fall at higher temperatures and that, as a result, chemical yield is lower at any particular size (as with high OA concentrations). However, at longer times, chemical yield can reach higher values because temperature dramatically affects growth rate (Figure 6c), and a larger amount of precursor is consumed during the growth phase. In fact, use of high temperature not only increases the average particle size at any given time but ultimately allows growth of sizes not practically reachable with HDD at lower temperatures, regardless of OA concentration. As with the OA experiments, injection temperature has a negligible effect on NQD size dispersion (Figure 6d), despite differences in growth rate.

Thus, the HDD-assisted growth demonstrates essentially the same temperature effects as previously reported syntheses.[28] As mentioned above, these trends are in opposition to numerical predictions. Though consistent, the origin of the discrepancy between simulation and experiment is not completely clear. It is logical that higher temperatures should increase the rate of monomer formation at injection, but this does not appear to result in a larger number of nuclei, as indicated by NQD concentration. This would suggest that the degree of supersaturation is not directly dependent on monomer concentration alone. Supersaturation level, by definition, is the amount by which the actual concentration exceeds the equilibrium concentration. Actual monomer concentration should increase at high injection temperatures, although when the reduction pathway is available (with HDD, DPP, or impure TOP) this increase may not be that dramatic. At the same time, the equilibrium concentration should also increase (as a rule), especially in the presence of sufficient stabilizing ligand. In our experiment, when strong, chelating donors outnumber metal species by 3:1, it is quite possible that at high temperatures the equilibrium can be strongly shifted away from nucleation (i.e., the equilibrium monomer concentration is higher), reducing the level of supersaturation and suppressing nucleation. As the growth phase begins, more monomer remains in solution, resulting in faster growth and larger NQDs.

HDD-Assisted Synthesis: Conditions for Size Control. Taken as a whole, the above experiments show that HDD can be used as a reducing agent in the synthesis of high-quality PbSe NQDs over a wide range of sizes. Increasing amounts of HDD lead to higher chemical yield up to roughly equimolar levels relative to lead, but in general, HDDs' effect on size and size distribution is fairly weak; thus, size-controlled synthesis depends on adjusting other parameters. To some extent, OA concentration can be used to tune size, but increased OA levels necessarily come at the cost of lower chemical yield. This is less the case with higher temperatures, however, which becomes the method-of-choice for reaching larger sizes. In light of these observations, in Table 1, we list the optimal parameters for the HDD-assisted synthesis of NQDs of four distinct sizes. These conditions were

Table 1. Specific Parameters for HDD-Assisted Synthesis of a Range of NQD Sizes, Using 1 mmol of Lead Acetate and 4 mmol of HDD

1S (nm)	radius (nm)	chemical yield(%)	PL QY(%)	σ (%)	OA (mmol)	$temp_{injection}$	growth time
1000	1.2	5	100	2.3	2.2	160 °C	10 s
1498	2.4	16	100	2.3	2.2	160 °C	50 min
2017	3.8	24	59	2.5	3.0	240 °C	15 min
2680	6.1	94	14	3.2	3.0	240 °C	2 h

verified using 4 mmol of HDD (i.e., a HDD/Pb ratio of 4:1), but reducing the amount down to 1 mmol results in very little change.

Theoretical Model and Numerical Simulation. In order to probe whether an additional monomer formation pathway can account for the effects of DPP or HDD on NQD growth, we carried out numerical simulation on NQD growth dynamics by methods similar to previous reports.[9,12,43] Our simulation encompassed the three initial steps of monomer generation, nuclei formation, and particle growth both with and without a reducing agent. Without a reducing agent (e.g., HDD), monomer generation proceeds by a single pathway (eq 1), and the rate can be expressed by eq 4 as a function of Pb^{2+} and Se concentrations. In the presence of HDD, we must also consider the contribution from the second, considerably faster pathway (eq 3).[44]

$$d[M_{PbSe}]_a/dt = v_1 = k_1[Pb^{2+}]^{\alpha 1}[Se]^{\beta 1} \quad \text{for eq 1} \tag{4}$$

$$d[Pb^0]/dt = v_2 = k_2[Pb^{2+}]^{\alpha 2}[HDD]^{\beta 2} \quad \text{for the first step of eq 3} \tag{5}$$

$$d[M_{PbSe}]_b/dt = v_3 = k_3[Pb^0]^{\alpha 3}[Se]^{\beta 3} \quad \text{for the second step of eq 3} \tag{6}$$

In eqs 4−6, $[M_{PbSe}]_a$ represents the concentration of PbSe monomer formed by direct reaction of Pb^{2+} with Se, and $[M_{PbSe}]_b$ represents the concentration of monomer formed in the Pb^0 reaction. Our model considers the combined monomer concentration over time of NQDs produced by both reaction pathways. In the second step, the rapid increase in monomer concentration constructs a supersaturation condition, under which nuclei are generated. Talapin et al. initially fixed the number of NQDs and the nuclei radius in the first modeling on NQD growth. In a later study, Hyeon et al. showed that the number of nuclei resulting from a reaction-created supersaturation could be successfully included in the simulation. From this consideration of the chemical reaction, nuclei are generated as follows:[43,45]

$$\frac{dN}{dt} = A\exp\left(-\frac{16\pi\gamma^3 {V_m}^2}{3{k_B}^3T^3{N_A}^2(\ln S)^2}\right) \tag{7}$$

$$S = [M_{PbSe}]_{a+b}/[M_{PbSe}]_{eq} \tag{8}$$

where N is the number of nuclei, A is a pre-exponential factor, V_m is the molar volume of crystal, k_B is the Boltzmann constant, T is temperature, and N_A is Avogadro's number. Supersaturation, S, is defined in eq 8 as the ratio between the actual PbSe monomer concentration and the equilibrium concentration. This expression, however, does not describe nuclei radius. To model the third step, growth, it is necessary to consider this size because NQD growth dynamics strongly depend on both particle size and concentration. For this purpose, we use the following expression:[46,47]

$$r_c = \frac{2\gamma V_m}{RT\ln S} \tag{9}$$

where r_c is the critical radius with zero growth rate, above which nuclei participate in growth and below which dissolution is the dominant process (i.e., the nuclei revert back to monomers). During growth, particles were considered to experience growth or dissolution depending on their surface potential under the corresponding supersaturation conditions according to eq 10.

$$\frac{dr}{dt} = V_m D[M]_{eq}\left(\frac{S - \exp\left(\frac{2\gamma V_m}{rRT}\right)}{r + \frac{D}{k_P^\circ}\exp\left(\alpha\frac{2\gamma V_m}{rRT}\right)}\right) \tag{10}$$

In the simulation, precursor concentration and supersaturation were calculated stepwise, and at each step, these conditions were used to generate the mean radius of nuclei, nuclei generation rate, and particle growth rate. The calculation was repeated 10^4 times to relate NQD concentration, supersaturation level, particle size and growth rate to dimensionless time for the reaction with and without HDD (Figure 7).[48]

Figure 7a depicts the effect of HDD on both monomer concentration and supersaturation level over reaction time. Initially, we see steep increases, indicating monomer formation, followed by fast decreases during nucleation. This is predicted by our simple picture of colloidal growth, as nucleation leads to a sudden decrease in supersaturation, conditions under which overproduced NQDs with small radii dissolve away. With HDD (red traces), the fast monomer generation rate causes two distinct and observable effects that can be verified experimentally. The first is a much larger nucleation event relative to the pure TOP case (black traces), indicated by the larger, sharper decline in both concentration and supersaturation, which is reflected in the much higher chemical yield of the HDD synthesis (Figure 2a). Second, the simulation predicts that the time lag between injection and nucleation will be shorter with HDD, a conjecture that can be easily verified qualitatively during sequential syntheses. In synthesis with only purified TOP, no color change is observed for up to 10 s after injection. In the presence of HDD, however, the reaction mixture turns dark brown nearly immediately after injection.

Figure 7b illustrates radius evolution over time. In addition to the general trend of reaching larger NQD sizes without HDD (black trace), the simulation predicts an interesting "crossover" in the growth curves at early times. This is due to the earlier onset of nucleation for the HDD synthesis (red) and its effects on the evolution of supersaturation. In Figure 7c, we show the simulated effects of supersaturation level on growth rate for a range of NQD radii. As we would expect, higher supersaturation results in faster growth. Because of the earlier, larger nucleation

(45) Mullin, J. W. *Crystallization*, 4th ed.; Oxford University Press: Oxford, 2001.

(46) Nielsen, A. E. *Kinetics of Precipitation*; Oxford: New York, 1964.

(47) Nuclei are generated with a normal distribution and the relative standard deviation of 15%.

(48) Simulated volume was 1.0×10^{-15} L, and injection temperature and growth temperature in simulation are 433 and 393 K. Parameters are fitted as follows: $\gamma = 0.08$ J m^{-2}, $A = 1.0 \times 10^{14}$ mol L^{-1} s^{-1}, $D = 1.0 \times 10^{-15}$ m^2 s^{-1}.

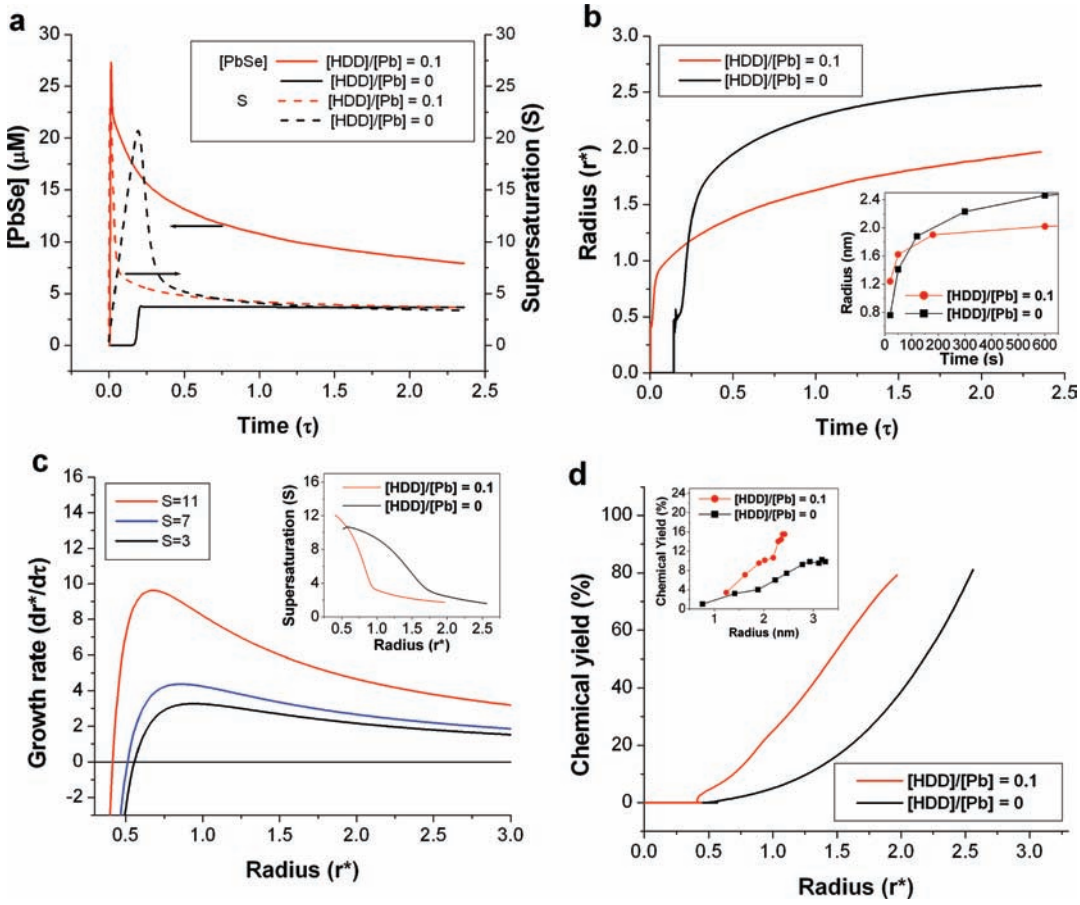

Figure 7. Simulation results for HDD-assisted synthesis of PbSe NQDs. [HDD]/[Pb] ratios of 0 and 0.1 are compared at an injection temperature of 160 °C, followed by growth at 120 °C. (a) Plot of NQD concentration and supersaturation as a function of dimensionless time (τ). (b) NQD radius as a function of dimensionless time (τ). (c) Growth rate as a function of dimensionless radius (r^*). Inset shows the simulation result of the change of supersaturation during NQD growth. (d) Chemical yield as a function of dimensionless radius (r^*). Inset shows experimental results. Dimensionless time (t) and radius (r^*) are defined as follows:[9] $\tau = (R^2T^2D[\mathrm{M}]_{\mathrm{eq}}t)/(4\gamma^2V_{\mathrm{m}})$ and $r^* = (RTr)/(2\gamma V_{\mathrm{m}})$.

event observed in the HDD synthesis, the corresponding supersaturation level is diminished relative to pure-TOP synthesis levels throughout the growth phase (inset of Figure 7c) and particularly at early times. Consequently, although growth starts earlier for HDD syntheses, the growth rate is lower, resulting in the observed crossover. This prediction can also be verified by experiment: the inset of Figure 7b depicts experimental data at early reaction times, demonstrating this same behavior in the real system. Similar correspondence can also be seen in comparing chemical yield as a function of radius (Figure 7d), where the model successfully captures the quick divergence between HDD and non-HDD synthesis in experiment.

Conclusion

While DPP can, as previously reported, increase chemical yield of the standard synthesis of PbSe NQDs, we find that use of HDD instead allows similar gains in chemical yield with better size control and higher PL QYs, particularly at larger sizes. These can be attributed to generally slower growth, which makes reaction timing more reliable and allows for better surface reorganization over the course of the reaction. In further studies of this new reaction system, we find that increased concentration of OA, as a strong-binding ligand, can inhibit nucleation, possibly through interfering with fast monomer generation. This results in larger NQDs but reduced chemical yield. Increased temperatures also reduce the size of the nucleation event, which we propose may be a result of increasing the equilibrium concentration of monomers relative to nuclei. At high temperatures, faster growth is observed, allowing one to produce even larger particles. While chemical yields for a given size are lower at high temperature, the reaction becomes fairly efficient at higher sizes. Finally, we found that numerical simulation based on a new, faster monomer generation pathway yields numerous predictions that can be verified experimentally. Overall, both our experimental and modeling studies support the view that reducing agents in general can effectively increase the efficiency of the PbSe NQD synthesis, but that somewhat weaker reducing agents like HDD result in a slower, more controllable reaction, yielding higher quality NQDs over a larger range of sizes. In this light, we offer this method as a promising approach to reproducible synthesis of high-quality PbSe NQDs in high chemical yield.

Acknowledgment. This work was supported by the Chemical Sciences, Biosciences, and Geosciences Division of the Office of Basic Energy Sciences, Office of Science, U.S. Department of Energy. V.I.K. acknowledges the support of the Center for Integrated Nanotechnologies, a U.S. Department of Energy Office of Basic Energy Sciences Nanoscale Science Research Center.

JA903445F